

**Chapter two**  
**Literature review**  
**Part one**

**2.1.1 Ionizing radiation**

Ionizing radiation is a broad energetic spectrum of electromagnetic waves or high velocity atomic or subatomic particles. The radiation can be categorized according to their ability to ionize the media. Non-ionizing radiation is electromagnetic radiation that does not have sufficient energy to remove an electron of the atom. The various types of non-ionizing radiation are ultra violet (UV), visible light, infrared (IR), microwaves (radio and television), and extremely low frequency (ELF, or as they called EMF or ELF-EMF). Ionizing radiation is electromagnetic radiations, such as X-rays,  $\gamma$ -rays and charged particles (electrons,  $\alpha$ -particles and  $\beta$ -particles) which possess sufficient energy to ionize an atom by removing at least an orbital electron. According to the 1996 European Guideline of the European Atomic Energy Community (EURATOM), electromagnetic radiation with a wavelength of 100 nm or less is considered as ionizing radiation which is corresponds to ionizing potential of 12.4 eV or more (Smith, 2000). The ionization potential is dependent on the electronic structure of the target materials and generally in the order of 4 – 25 eV.

The International Commission of Radiation Units (ICRU) has subdivided the ionizing radiation into direct and indirect ionizing radiation, based on the mechanisms by which they ionized the atom. Direct ionizing radiations are fast charged particles, such as alpha particles, electrons, beta particles, protons, heavy ions, and charged mesons, which transfer their energy to the orbital electron directly and ionize the atom

by means of Columbic force interactions along their track. Indirect ionizing radiations are uncharged quantum, such as electromagnetic radiations (X-rays and  $\gamma$ -rays), neutrons, and uncharged mesons, which undergo interactions with matter by indirectly releasing the secondary charged particles which then take turn to transfer energy directly to orbital electrons and ionize the atom. Some properties of ionizing radiation are shown in Table 2.1.1

**Table 2.1.1 shows the properties of different ionizing radiation**

Characteristics	Alpha	Proton	Beta or electron	Photon	Neutron
Symbol	or ${}^4_2\alpha$ He <sup>+2</sup>	or H <sup>+1</sup> <sub>1</sub> p	or $\beta_{-1}e$	$\gamma$ - or X-rays	${}^1_0n$
Charge	+2	+1	-1	Neutral	Neutral
Ionization	Direct	Direct	Direct	Indirect	Indirect
Mass (amu)	4.00277	1.007276	0.000548	-	1.008665
Velocity (m/s)	6.944 x10 <sup>6</sup>	1.38 x10 <sup>7</sup>	2.82 x10 <sup>8</sup>	2.998 x10 <sup>8</sup>	1.38 x10 <sup>7</sup>
Speed of light	2.3%	4.6%	94%	100%	4.6%
Range in air	0.56 cm	1.81 cm	319 cm	820 m	39.25 cm

**1 atomic mass unit (amu) = 1.6 x 10<sup>-27</sup> kg. Speed of light c = 3.0 x 10<sup>8</sup> m/sec.**

### 2.1.2 Radiation sources

The sources of ionizing radiation can be divided into two categories namely as natural and man-made sources. The first natural sources are cosmic radiation which is the radiation coming from outside our solar system as positively charged ions (protons, alpha, heavy nuclei) and interact with atmosphere to produce secondary radiations such as x-rays, muons, protons, alpha particles, pions, electrons and neutrons. The second

natural sources are external terrestrial sources which represent the radioactive materials found naturally in the earth crust, rocks, water, air and vegetation. The major radionuclides found in the earth crust are Potassium-40, Uranium-235, and Thorium-232. The main sources of man-made radiations that expose the public are in the form of medical diagnostic X-ray, radiation therapy, nuclear medicine and sterilization. The common radioactive sources are  $^{131}\text{I}$ ,  $^{99\text{m}}\text{Tc}$ ,  $^{60}\text{Co}$ ,  $^{192}\text{Ir}$ ,  $^{90}\text{Sr}$  and  $^{137}\text{Cs}$ . Other man-made sources exemplar in occupational and consumption products that originated in mines, combustible fuel (gas, coal), ophthalmic glasses, televisions, luminous watch's dial (tritium), X-rays at the airport (scanner), smoke detectors (Americium-241) and fluorescent lamp starters, nuclear fuels, nuclear accidents and nuclear weapons.

The yield of artificial sources is represented either as quantum in X-rays and  $\gamma$ - rays or as high energy particles such as beta particles ( $\beta$ ), alpha particles ( $\alpha$ ), neutrons and electrons (Smith, 2000). Most of the types of radiation source discussed above are used in medicine, industry, and research. Today the most common radiation sources used is  $^{60}\text{Co}$ , which is an artificial source of  $\gamma$  radiation and linear accelerators for photon and electron beams having potential energy ranging from 0.3-10 MeV to 20 MeV. Table 13.2 shows the radiation sources commonly used in industry and research.

**Table 2.1.2 shows the common sources of ionizing radiation. (Smith, 2000)**

Category	Source
Nuclear power	$^{235}\text{U}$ fission products, $^{90}\text{Sr}$ , $^{137}\text{Cs}$
Occupational exposure	X-ray, isotopes for $\gamma$ - rays
Weapons tests	$^{235}\text{U}$ , $^{239}\text{Pu}$ , fission products
Every day sources	Coal, Tobacco and Air-travel
Medical tests & treatment	X-ray, $\gamma$ -rays & electrons
Cosmic rays	Protons, electrons, neutrons
Food	$^{40}\text{K}$ , $^{137}\text{Cs}$ , $^{14}\text{C}$ and $^{131}\text{I}$
Rocks & building	$^{235}\text{U}$ , $^{238}\text{U}$ , and $^{232}\text{Th}$
Atmosphere	$^{222}\text{Rn}$ and $^{137}\text{Cs}$

### 2.1.3 $\gamma$ - radiation sources

$\gamma$ -rays are produced by the nuclear transitions that occur within the nuclei of radioactive elements. The emitted photons are mono-energetic with specific energy to the isotope from which they originate. By far the most commonly employed radioactive isotope for  $\gamma$ -rays is cobalt-60 ( $^{60}\text{Co}$ ), an isotope with a half-life of 5.272 years.  $^{60}\text{Co}$  emits two  $\gamma$ -photons of equal intensity at 1.17 and 1.33 MeV. It is produced in nuclear reactors by a neutron-capture reaction involving  $^{59}\text{Co}$ . Due to the long half-life, high penetrating power and ease of production,  $^{60}\text{Co}$  sources have become sources of choice in both industrial and research institutions. The activity of the sources prepared in nuclear reactors can be made high up to 40 Ci/g (1.5 TBq/g), however sources with activity from 1 to 5 Ci/g are typically common for use. Over 80% of the  $^{60}\text{Co}$  produced worldwide is manufactured by the Canadian company, Ontario Hydro and marketed by another Canadian company, MDS Nordion.

$^{60}\text{Co}$  radioisotope decays to stable nickel-60 by a nuclear transition ( $\beta$ -decay) in which a neutron is converted into a proton via the emission of a  $\beta$ -particle with energy of 312 keV and two  $\gamma$ -photons, one of 1.17 MeV and another of 1.33 MeV. The decay scheme of this isotope is illustrated in Figure 2.1.1 (Choppin et al., 1995; Attix, 1986).

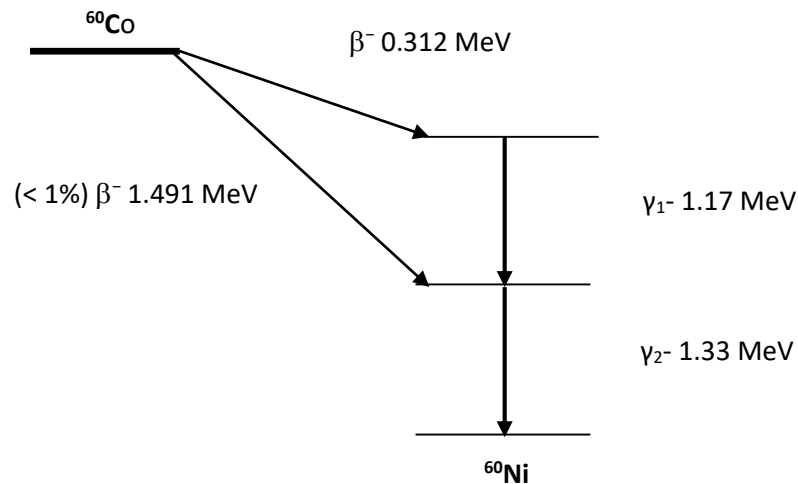


**Figure 2.1.1** Decay scheme of  $^{60}\text{Co}$  radioisotope which ends by Nicle-60 stable. Another frequently used  $\gamma$ -ray source is cesium-137, a fission product from nuclear reactors. The energy of the emitted photon is 662 keV and the half-life is 30.17 years. Nuclear reactors themselves are potential sources of  $\gamma$ -rays.

### 2.1.4 $\gamma$ -radiation interaction with matter

When photons of  $\gamma$ -radiation interact with matter, they undergo attenuation and hence lose their energy and intensity by the process of photoelectric absorption, Compton inelastic scattering, pair production, and Rayleigh elastic scattering (Evan, 1952).

#### 2.1.4.1 Photoelectric absorption

Absorption of  $\gamma$ -rays occurs when the  $\gamma$ -ray photon is absorbed by an electron resulting in ejection of the electron from the inner shell of the atom and ionization of atom take

place. Subsequently, the ionized atom returns to the neutral state with the emission of characteristic X-ray of the atom shown in Figure 2.1.1 This subsequent emission of lower energy photons is generally absorbed and does not contribute to (or hinder) to the secondary ionization. Photoelectron absorption is the dominant process for  $\gamma$ -ray absorption up to energies of about 500 keV. The photoelectric absorption process predominates for photons in the low energy range between 10 keV and 200 keV. This is the phenomenon explained by Einstein in 1905, in which an incident photon gives up all its energy  $h\nu$  to a bound electron, usually K shell (90%), where subsequently part of the energy is used to overcome the electron binding energy  $E_B$  and the extra energy is converted as kinetic energy  $K_E$  of the photoelectron. This can be expressed in equation (2.1.1).

$$h\nu = K_E + E_B \quad (2.1.1)$$

The atom that is left in an excited state will emit fluorescent x-rays or Auger electrons. The characteristic X-rays may escape especially for high-energy photons and high atomic number of absorbing material unless the absorber is thick enough to stop the  $\gamma$ -rays. The ranges of the Auger electrons are short and locally absorbed. The cross-section for photoelectric effect in K shell of an atom with atomic number  $Z$  for photon energy  $h\nu$  is given by equation (2.1.2), from which we could deduce that the photoelectron absorption is dominant for atoms of high atomic numbers and for photon of low energy..

$$\sigma_K = \varphi_0 4\sqrt{2} \left( \frac{m_0 c^2}{h\nu} \right)^{7/2} \frac{Z^5}{137^4} \quad (2.1.2)$$

where  $\varphi_0 = \pi r_0^2$  and  $r_0 = e^2 / m_0 c^2 = 2.818 \times 10^{-15} m$  is the classical electron radius,  $m_0$  is the rest mass of electron and  $c$  is the speed of light.  $m_0 c^2$  is the rest energy of the recoil

electron, according to mass-energy equation proposed by Einstein in 1905 in the relativity theory.

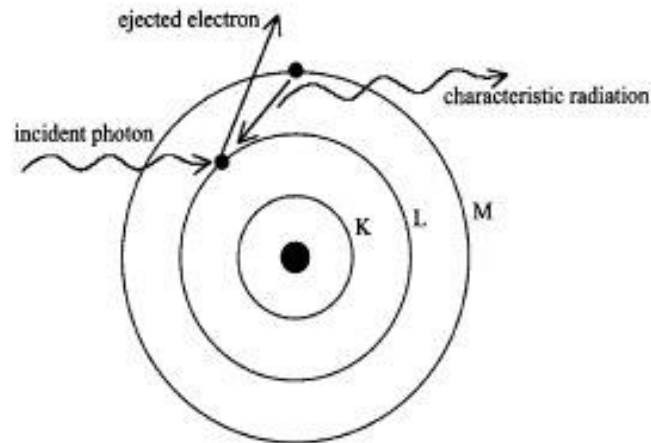


**Figure 2.1.2** Schematic diagram of photoelectric absorption of  $\gamma$ -radiation resulting in ejection of orbital electron from L shell leading to ionization process of an atom.

#### 2.1.4.2 Compton Scattering

Compton scattering process also known as an incoherent scattering, occurs when the incident photon ejects free or weakly bonded electron from an atom and a photon of lower energy is scattered from the atom. Relativistic energy and momentum are conserved in this process and the scattered  $\gamma$ -ray photon has less energy and therefore greater wavelength than the incident photon shown in Figure 2.1.3. Compton scattering is important for low atomic number specimens. At energies of 100 keV - 10 MeV the absorption of radiation is mainly due to the Compton effects (McGervey, 1983). The change in wavelength of the scattered photon is given by equation (1.3)

$$\frac{c}{\nu'} - \frac{c}{\nu_0} = \lambda' - \lambda_0 = \frac{h}{mc(1 - \cos \theta)} \quad (2.1.3)$$

where  $\lambda$  is the wavelength of the incident photon,  $\lambda_0$  the wavelength of the scattered photon,  $m$  is the mass of the electron and  $\theta$  the angle of scattering for the photon. On rearranging, the above equation we got the following equation (1.4)

$$h\nu = \frac{h}{1 + \alpha(1 - \cos \theta)} \quad (2.1.4)$$

Where is the ratio of the energy of the photon to the rest energy of the electron i.e.

$\alpha = h\nu/m_0c^2$ . The kinetic energy  $T$  for the recoil electron is given by equation (1.5)

$$T = h\nu \frac{\alpha(1 - \cos \theta)}{1 + \alpha(1 - \cos \theta)} \quad (2.1.5)$$

And the scattering angle of the electron is given by equation (1.6)

$$\cot \phi = (1 + \alpha) \tan \frac{1}{2} \theta \quad (2.1.6)$$

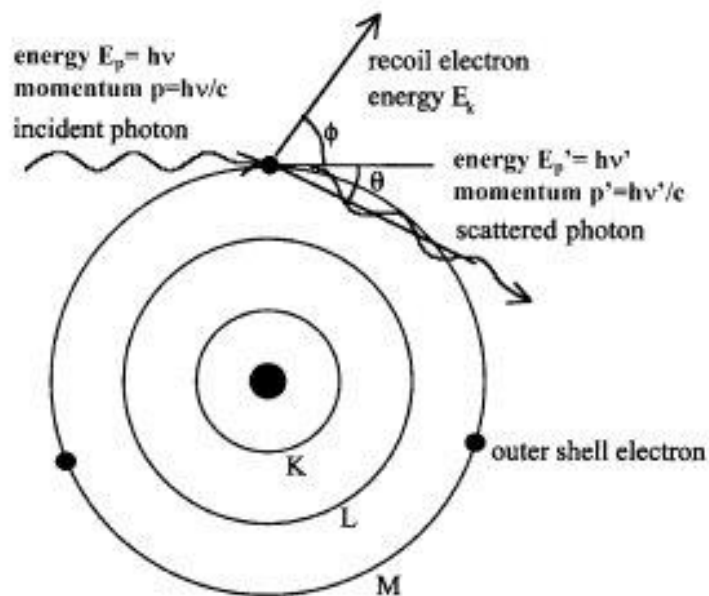


**Figure 2.1.3 Schematic diagram of Compton scattering for  $\gamma$ -radiation resulting in ionization and scattering of the incident photon with less energy**



### 2.1.4.3 Pair Production

The production of a positive and negative electron pair (pair production) is a process that can take place in the vicinity of the nucleus field of an atom or an electron field. Absorption of photons through the mechanism of pair production can occur when the energy of an incident photon is greater than twice the rest mass of an electron, i.e.  $2m_0c^2 = 1.022 \text{ MeV}$  (Johns and Cunningham, 1983). During pair production interactions, a photon has its energy converted to an electron–positron pair. The positron so produced interacts with matter by ionizing and exciting atoms through the same processes as electrons, thus losing energy and being brought to rest. At this point, the positron combines with an electron in an annihilation process producing two photons with energy equal to 0.511 MeV as shown in Figure 2.1.4.

Pair production is an absorption process in which a photon in the field of nucleus produces an electron-positron pair, where the total kinetic energy is equal to the energy of photon minus the rest energy of the two particles, which have been created as shown in equation (2.1.7), thus the photon energy must be greater than 1.02 MeV for the interaction to take place. The electron and positron do not necessarily receive equal energy, but their average energy is given by equation (2.1.8).

$$h\nu = (m_0c^2 + T_-) + (m_0c^2 + T_+) \quad (2.1.7)$$

$$\bar{T} = \frac{h\nu - 1.022}{2} \text{ MeV} \quad (2.1.8)$$

The cross-section of the pair production in the field of nucleus is given by equation (2.1.9)

$$\sigma_{PP} = \frac{1}{137} r_0^2 Z^2 \left[ \frac{28}{9} \ln \left( \frac{2h\nu}{m_0 c^2} \right) - \frac{218}{27} \right] \quad (2.1.9)$$

The triplet production process is similar but the interaction takes place with one of the atomic electrons which receives sufficient energy to be set free. It occurs when the incident photon have an energy of  $4m_0c^2$ , i.e. it implies both the pair production at the nucleus level plus triplet production. The total kinetic energy is equal to the energy of photon minus the rest energy of the three ejected particles as given by equation (2.1.10), from which the average kinetic energy can be deduced by equation (2.1.11) (Motzet *al.*, 1969)

$$h\nu = (m_0c^2 + T_-) + (m_0c^2 + T_+) + (m_0c^2 + T_*) \quad (2.1.10)$$

$$\bar{T} = \frac{h\nu - m_0c^2}{3} \text{ MeV} \quad (2.1.11)$$

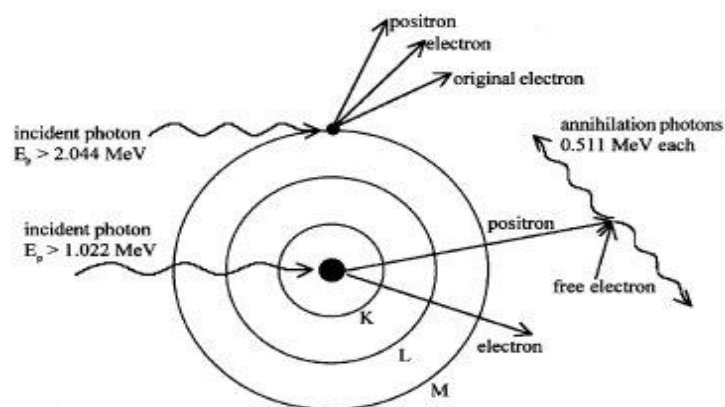


**Figure 2.1.4** Schematic diagram of Pair Production process for  $\gamma$ -radiation being interfered in the nucleus field and orbital electron to produce triplet particles.

#### 2.1.4.4 Raleigh scattering

The coherent Rayleigh scattering by an atom is predominant for photons at low energy range from 1 keV to 100 keV. The Rayleigh scattering is a process in which a photon is deflected by a bounded electron of the atom and photon going off in different directions with no loss in energy. The atomic system may recoil as a whole under impact without the atom being ionized or excited. The probability of this process is large only for low energy photons and high atomic number material. The differential cross-section of the coherent scattering of photon at deflection angle  $\sigma$  by a bounded electron is given by equation (2.1.12)

$$d\sigma_{coh} = \frac{1}{2} r_0^2 (1 + \cos^2 \theta) \left[ \frac{F(\alpha, \theta, Z)^2}{Z} \right] d\Omega \quad (2.1.12)$$

Where  $F(\alpha, \theta, Z)$  is the atomic form function which varies from zero at large angle to  $Z$  at the smaller angle.

#### 2.1.5 $\gamma$ -ray attenuation coefficients

In general, the characteristic of radiation interaction with matter is that each individual photon is absorbed or scattered from the incident beam in a single event. The photon number  $I_0$ , i.e.  $\Delta I = -\mu I_0 \Delta x$ , where,  $\mu$  is a constant proportionality called the attenuation coefficient. In this case, upon integrating, we have the following equation (2.1.13)

$$I = I_0 e^{-\mu x} \quad (2.1.13)$$

The attenuation coefficient is related to the probability of interaction per atom, i.e. the atomic cross section  $\sigma_a$  is given by equation (2.1.14)

$$\mu = \frac{\sigma_a N_A \rho}{A} \quad (2.1.14)$$

Where  $A$  is the mass number and  $N_A$  the Avogadro's number ( $6.022 \times 10^{23}$  mol/l), Table 2.1.3 briefly summarized the entire  $\gamma$ -radiation photon interactions with their possible energies required to initiate the reactions (Smith, 2000; Siegbahn, 1965).

### **2.1. 6 $\gamma$ -radiation interaction with molecules**

The essence of  $\gamma$ -radiation interaction with molecules and change the physical and chemical characteristics of the formed compound is ascribed to the amount of energy being transferred, which will create ion, free radicals and excited molecule. Such interaction process is termed ionization and excitation of the molecules, which can cause chemical changes to the irradiated molecule. This is due to the fact that all binding energy for organic compound in the range of 10 – 15 eV. In case of low transferred energy by photon, the molecule undergoes excitation state before returning to the rest state by emitting X-ray photons or break down to release free radicals which in turn undergoes polymerization.

The ejected electron from the irradiated molecule ( $A^+$ ) is subjected to the strong electric field of the formed positive charge. Therefore the recombination is a frequently occur, either during irradiation or after the end of irradiation to create energetic molecule ( $A^{**}$ ). Such highly energetic excited molecule will break down into free radicals and new molecule (Denaro, 1972). The fundamental of this reaction can be shown in the following scheme Figure 2.1.5

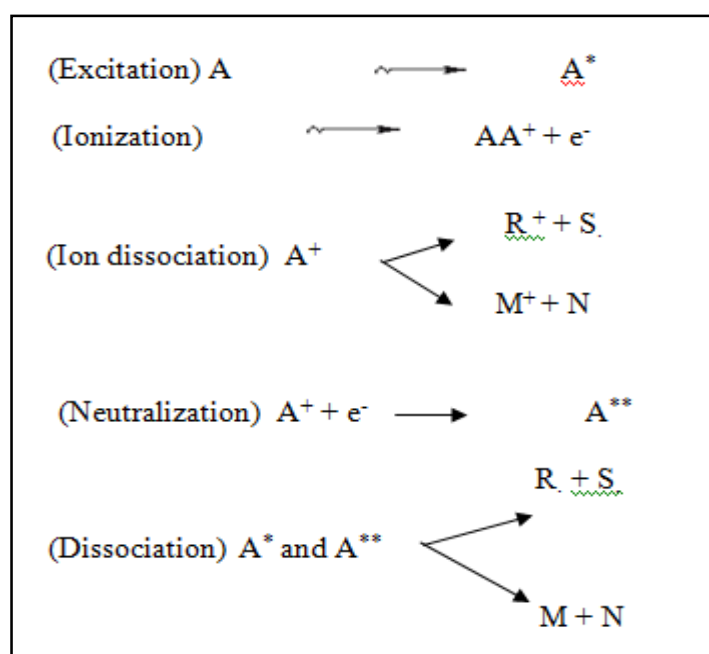


**Figure 2.1.5 shows the expected irradiation results of the organic molecules, where R. and S. are free radicals and M and N are molecular products.**

### 2.1.7 Polymerization

Radiation polymerization is a process in which the free radicals interact with the unsaturated molecules of a low molecular unit known as monomer to form high molecular mass polymer or even with different monomers to produce crosslink polymer. The formed polymer can be in different forms called homopolymer and copolymer depending on the monomer compositions link together.

Radiation-induced polymerization process can be achieved in different media whether it is liquid or solid unlike the chemical polymerization which can only be accomplished in aqueous media. It is also temperature independent. Radiation polymerization often continues even after removing away from the radiation source. Such condition is known as post-polymerization (Lokhovitsky and Polikarpov, 1980).

Since radiation initiation is temperature independent, polymer can be polymerized in the frozen state around aqueous crystals. The mechanism of the radiation induced polymerization is concerning the kinetics of diffusion-controlled reactions and consists of several stages: addition of hydroxyl radicals and hydrogen atoms to carbon-carbon double bond of monomer with subsequent formation of monomer radicals; addition of hydrated electrons to carbonyl groups and formation of radical anion of a very high rate constant and the decay of radicals with parallel addition of monomer to the growing chain.

#### **2.1.7.1 Cross linking**

The process of crosslink occurs due to interaction between two free radical monomers which combine to form intermolecular bond leading to three dimensional net of cross-linked highly molecular polymer, more likely dominate in unsaturated compound or monomer. The cross-linked polymer shows strong mechanical strength and high thermal resistance.

### **2.1.7.2 Radiation grafting**

Radiation grafting is a process in which active radical sites are formed on or near the surface of an existing polymer, followed by polymerization of monomer on these sites. Grafting is accompanied by homo-polymerization of the monomer; the material to which the monomer is grafted is described as the backbone, trunk or support.

Radiation grafting is used to modify the polymers texture such as film, fibers, fabrics and molding powders.

The process of grafting can be expressed as follow; suppose the polymer A is exposed to  $\gamma$ -rays, thus the active free radical sites  $A^*$  created randomly along the polymer backbone chain, this free radical initiate a free radical on the monomer B then undergoes grafting polymerization at that active sites. The extension of the attached monomer B upon the base polymer A is termed as the degree of grafting DOG which refers to the mass of the grafted polymer as a percentage of the mass of the original base polymer. Such process can be expressed in schematic Figure 2.1.6.

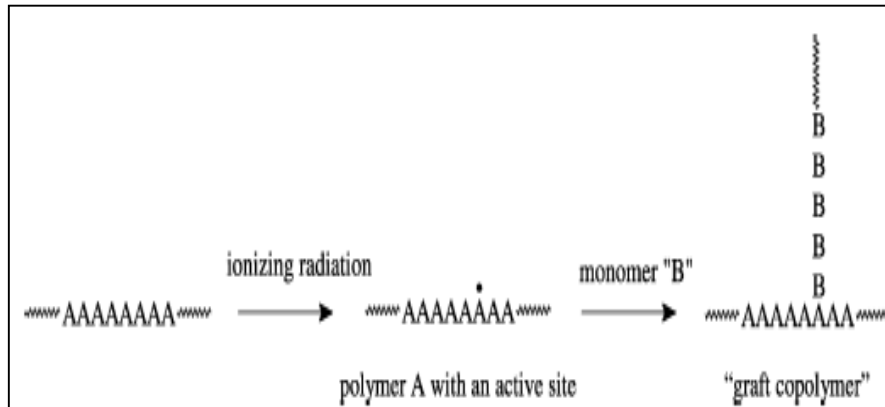


Figure 2.1.6 shows the schemes for grafting process for polymer A with monomer B using  $\gamma$ -radiation.

## 2.1.8 Absorption of light and UV-Visible spectrophotometry

### 2.1.8.1 Optical absorption

The transmittance of light across the absorber accompanied with absorption of the light waves. Such absorption depends on the wavelength of the light, thickness of the absorber or the transmitted media and the nature of the media. Beer-Lambert Law, successfully determined the absorption coefficient of the media as follows; supposing a light beam  $I$  is being incident to an object whose area is  $a$ ,  $\alpha$  is its absorption coefficient, then the fraction absorption  $dI$  of light by this absorber in a thickness  $dx$  is given by the following equation (2.1.15)

$$dI = -\alpha I dx \quad (2.1.15)$$

or 
$$\frac{dI}{I} = -\alpha dx \quad (2.1.16)$$



The integrating of this equation (2.1.16) gives the absorbance  $A$  as in equation (2.1.17). In this case the light intensity  $I$  changed from  $I_0$  to  $I$  by crossing a distance from  $x = 0$  to  $x = x$  in the absorber.

$$\int_{I=I}^{I=I_0} \frac{dI}{I} = -\alpha \int_{x=0}^{x=x} dx$$

$$\ln I / I_0 = -\alpha x$$

$$\ln(I) - \ln(I_0) = -\alpha x$$

$$\ln \frac{I}{I_0} = -\alpha x$$

$$\log \frac{I}{I_0} = e^{-\alpha x} = A \quad (2.1.17)$$

From equation (2.1.17) of absorbance  $A$ , the absorption coefficient  $\alpha$  can be deduced in equation (2.1.18).

$$\log \frac{I}{I_0} = \frac{\alpha x}{e^{-1}} = \alpha x$$

$$\frac{e \times A}{x} = \alpha \quad (2.1.18)$$

As the value of  $\log \frac{I}{I_0} = A$  and  $e$  is 2.303, then the absorption coefficient can be given by equation (2.1.19)

$$\alpha = \frac{2.303 \times A}{x} \quad (2.1.19)$$

Where  $x$  is the distance crossed by the light or can be the sample thickness in case of UV-visible spectroscopy. The corrected absorption value known as the molar

absorptivity ( $\epsilon$ ) is used for the comparison between different spectra of different compounds and can be expressed by the following equation:

$$\epsilon = \frac{A}{cl} \quad (2.1.20)$$

Where  $A$  = absorbance,  $c$  = sample concentration in moles/liter and  $l$  = path length through the cuvette in cm.

### **2.1.8.2 Mechanism of absorption process**

The absorption processes of microwaves in polymer, generally accompanied with energy reduction in the transition wave. Such reduction is due to the optical absorption constant of the media  $\alpha$  which come in the range of  $10^5 - 10^6 \text{ cm}^{-1}$  (Richard, 1988). The variation of the absorption on the transition involves a photon only (direct transition), or that involves both a photon and a phonon (indirect transition). As the photon energy drops below the band gap energy, the absorption constant decreases by many orders of magnitude.

The energy levels are created if imperfections are present in the polymers. They lie in forbidden gap. At energy less than the band gap energy it is still possible to excite electrons to the conduction band from imperfection levels occupied by electrons. Electrons also can be excited from the valence band to unoccupied imperfection levels. Each process will give rise to optical absorption. When the photon energy is less than the energy required to make a transition from the imperfection level to one of the bands, this absorption in turn comes to an end.

The corresponding absorption constant  $\alpha$  may have values as high as  $10^3 \text{ cm}^{-1}$  for very high imperfection densities, but in general is considerably less.  $\mu$ Absorption of photons by free carriers, cause a transition to higher energy states within the same band or to higher bands. This process can occur over a wide range of photon energies. It involves the absorption of both photons and phonons since both energy and  $k$  must be changed in the transition. There is also an optical absorption due to free carriers acting collectively as a kind of electron gas, which is known as plasma resonance absorption.

### **2.1.8.3 Absorption edge**

The transition of electrons between the valence and conduction bands in the polymers start at the absorption edge which refer to the minimum or threshold energy at which the absorption coefficient started. The transition is called direct if it is extreme occur due to direct absorption of the incident photonic energy, or can be indirect transition in case of phonon assisted initiation. Mostly all the materials have discriminated absorption edge and the energy gap  $E_g$ , which related to their chemical properties, hence such criteria can be utilized as a fingerprint in materials characterization (Tauc, 1974).

The absorption constant  $\alpha(\nu)$  within the range of  $\sim 1 \text{ cm}^{-1}$  up to  $10^4 \text{ cm}^{-1}$ , is described by the following equation (1.21)

$$\alpha(\nu) = \alpha_0 \exp \left( \frac{h\nu}{E_e} \right) \quad (2.1.21)$$

Where, the energy ( $E_e$ ) is the absorption edge in eV.

#### 2.1.8.4 Optical band gap

At high enough absorption levels ( $\alpha > 10^4 \text{ cm}^{-1}$ ), the absorption constant ( $\nu$ ) commonly take place as frequency dependence from which the band gap energy between the conductive band CB and the valence band VB can be deduced, depending on Mott and Davis (1979) which is applicable for UV-spectrum. It correlates between energy band gap  $E_g$  and the absorption coefficient  $\alpha(\nu)h\nu$  of the composites as in the following equation (1.22)

$$\alpha(\nu)h\nu = B(h\nu - E_g)^m \quad (2.1.22)$$

Where  $h\nu$  is the energy of the incidence photon,  $h$  is the Planck constant,  $E_g$  is the optical band gap energy,  $B$  is a constant known as the disorder parameter which is dependent on composite composition and independent to photon energy. Parameter  $m$  is the power coefficient with the value that determined by the type of possible electronic transitions, such as direct allowed and indirect allowed (Tauc, 1974). The direct transition is the transition of electron from the band  $i$  via  $k$  band to the final conduction band  $f$  by the transition-dipole moments and the electric fields at the surface, while the indirect transition the incident photon is absorbed in the substrate followed by scattering of a photo-excited electron trapped into the intermediate state  $k$  band then transfer to final band  $f$ , as being

illustrated in Figure (1.7). All the electrons of the valence band can connect to the empty states of the conduction band by indirect transition process; however, phonons, could also participate in the transition process (Pankove, 1971).

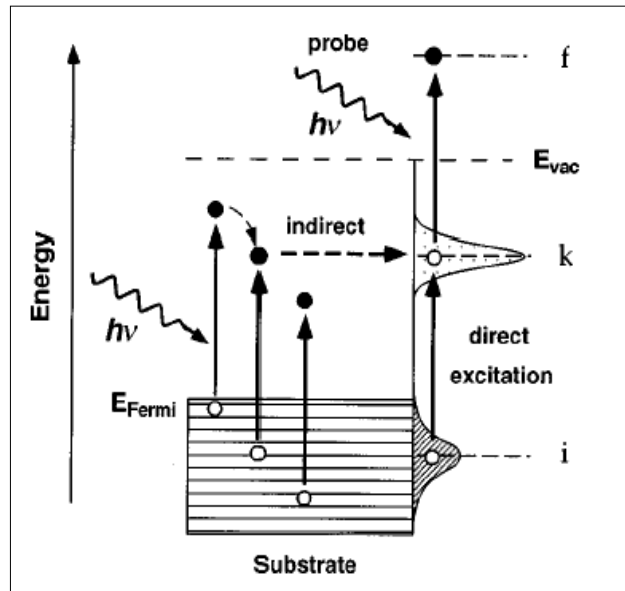


**Figure 2.1.7** Schematically illustrates the sequence of direct electronic transitions from the initial state  $i$  to the final state  $f$ , or by an indirect process in which the intermediate state  $k$  is populated by scattering and relaxation of “hot” electrons, which are photo-excited in the substrate.

### 2.1.8.5 UV-Visible absorption spectrophotometry

The following Figure (1.8) explains the UV-visible spectroscopy principle, in which a beam of light from a UV-visible light source is separated into its component wavelengths by a prism or diffraction grating. Each monochromatic (single wavelength) beam in turn is split into two equal intensity beams by a half-mirrored device. One beam for the sample (colored magenta), passes through a small transparent container (cuvette) as a sample chamber. The other beam, for reference (colored blue), passes through an identical cuvette. The intensities of

these light beams are then measured by electronic detectors and compared. The intensity of the reference beam, with no light absorption, is defined as  $I_0$  and the intensity of the sample beam is defined as  $I$ . Over a short period of time, the spectrometer automatically scans all the component wavelengths in the manner described. The UV region scanned is normally from 200 to 400 nm, and the visible portion is from 400 to 800 nm (Whiffen, 1971).

If the sample compound does not absorb light of a given wavelength, then  $I = I_0$ . However, if the sample compound absorbs light then  $I$  is less than  $I_0$ , and this difference may be plotted on a graph versus wavelength, as shown on the right. Absorption may be presented as transmittance ( $T = I/I_0$ ) or absorbance ( $A = \log I_0/I$ ). If no absorption has occurred,  $T = 1.0$  and  $A = 0$ . Most spectrometers display absorbance on the vertical axis, and the commonly observed range is from 0 (100% transmittance) to 2 (1% transmittance). The wavelength of maximum absorbance is a characteristic value, designated as  $\lambda_{\max}$ .

Different compounds have very different absorbance. The reference absorption intensity for the system is based on a completely transparent standard compound (non-absorbing). The most commonly used compounds are water, ethanol, hexane and cyclohexane. The compounds with double or triple bonds and heavy atoms are generally avoided, because the absorbance of a sample will be proportional to its molar concentration in the sample cuvette.

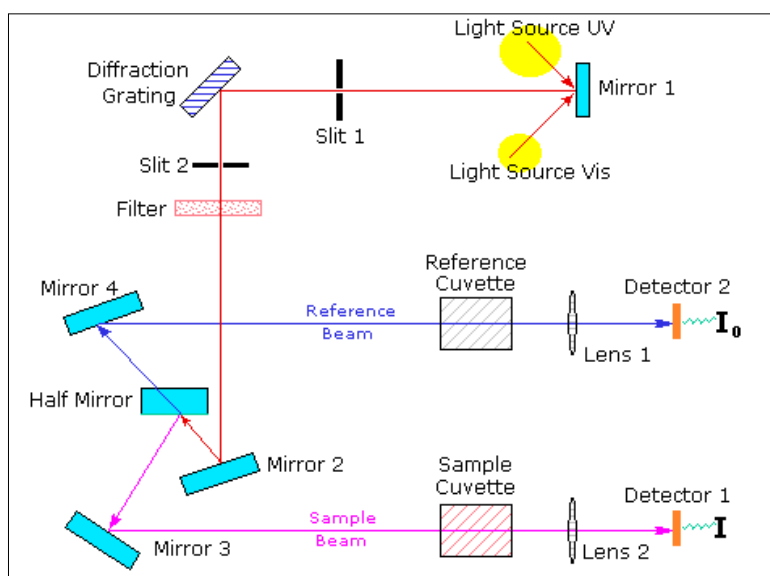


**Figure 2.1.8 Schemes for UV-visible spectroscopy principle and steps of taking the spectra.**

### 2.1.9 Radiation therapy dose

Measuring of dose is most important in radiation therapy because of the effect of radiation in the skin of the patient, and Prediction of skin reactions requires knowledge of the dose at various depths in the human skin. Using thermoluminescence dosimeters of different thicknesses, the dose can be extrapolated to the surface and interpolated between the different depths.

The thermo-luminescent (T.L.) phosphoric material such as LiF(Mg, Cu and P) which are usually named (TLD100H) has shown great interest of scientists in the field of radiation dosimetry due to its very favorable dosimetric characteristics

(Fung 2004). This material was first introduced in the powder form by Nakajima et al. in 1978 then the development continued and commercialized in 1990 as LiF:Mg,Ti (TLD100) and the LiF(Mg,Cu,P) T.L. phosphors which are tissue-equivalent. The TLD100H is considered as outperforms due to its very higher sensitivity, by a factor of greater than 25, and a dose detection threshold of less than 1 mGy (Moscovitch 1999). Therefore, TLD has been used in the field of radiation dosimeter and correlation of dose to biological effects (Ayad 2000).

One of the most promising realms being under focused by scientists in the nanocomposites materials which have many applications in the field of medical engineering, electronics, electrochemical, biosensors, radiation detection/measurements and optical/display systems that is for their wide range of absorption frequencies and ultrafast response behaviors (1). Nanocomposites materials categorized under nanotechnology which can be defined as the science dealing with the construction and use of functional structures designed from atomic or molecular scale which at least one characteristic dimension measurement in nanometers (Kensuke et al.,2000;Carl, 2002).

All metallic nanoparticles (Gold, Silver, Platinum...etc) exhibit unusual electrical, magnetic, optical and electrochemical properties due the near-free conduction electrons, which are depend on their size, surface Plasmon, surface



free energy and surface area, as well as on the surrounding dielectrics (Stakeev and Kustov, 1999).

The recent studies on polymer/silver nanocomposites revealed that the properties of silver within its composites answer many potential applications in optical waveguides, optical switches, molecular identification, oxidative catalysis, antimicrobial effects, etc.

These mentioned properties are dependent on the particle size, shapes and the method of composites synthesis. Varieties of synthesis methods have been developed, including reduction from metallic salts, ultrasonic irradiation technique, ion implantation, and thermal process and microwave technique. The synthesis of silver nanocomposites by using  $\gamma$ -irradiation has been mentioned by Ali et al., (2007). The radiation measurements in this study will depend on the optical density measurement and optical absorbance measurement using optical densitometer and UV-visible spectroscopy accordingly. Also the radiation effect on the Silver/ PVA composites will be shown out of SEM studies. The expected x-ray or  $\gamma$  exposure on the silver/PVA composites film will be as color change to yellow or golden due to presence of silver while the expected change on PVA will be as degradation of the PVA chain.

## **Chapter two**

### **Part two**

#### **2.2.1 Radiation dosimeters**

Radiation dosimeter is a device, instrument or system that measures or evaluates, either directly or indirectly, the quantities exposure, kerma, absorbed dose or equivalent dose, or their time derivatives (rates) or related quantities of ionizing radiation. A dosimeter along with its reader is referred to as a dosimetry system. Measurement of a dosimetric quantity is the process of finding the value of the quantity experimentally using dosimetry systems. The result of measurement is the value of a dosimetric quantity expressed as the product of a numerical value and an appropriate unit.

To function as a radiation dosimeter, the dosimeter must possess at least one physical effect that is a function of the measured dosimetric quantity and can be used for radiation dosimetry with proper calibration. In order to be useful, radiation dosimeters must exhibit several desirable characteristics. For example, in radiotherapy, the exact knowledge of both the absorbed dose to water at a specified point and its spatial distribution are of importance, as well as the possibility to derive the dose to an organ of interest in the patient. In this context, the desirable dosimeter properties will be characterized by accuracy and precision, linearity, dose or dose-rate dependence, energy response, directional dependence and spatial resolution.

Obviously, not all dosimeters can satisfy all characteristics, therefore, the choice of a radiation dosimeter and its reader must be made judiciously, taking into account the requirements of the measurement situation, e.g., in radiotherapy ionisation chambers are recommended for beam calibrations (reference dosimetry – see Chapter 9) and other dosimeters, such as those discussed below, are suitable for the evaluation of the dose distribution (relative dosimetry) or dose verification.

## **2.2.2 PROPERTIES OF DOSIMETERS**

### **2.2.2.1 Accuracy and precision**

In radiotherapy dosimetry the uncertainty associated with the measurement is often expressed in terms of accuracy and precision.

The precision of dosimetry measurements specifies the reproducibility of the measurements under similar conditions and can be estimated from the data obtained in repeated measurements. High precision is associated with a small standard deviation of the distribution of measurement results.

The accuracy of dosimetry measurements is the proximity of their expectation value to the ‘true value’ of the measured quantity. Results of measurement cannot be absolutely accurate and the inaccuracy of a measurement result is characterized as uncertainty.

The uncertainty is a parameter that describes the dispersion of the measured values of a quantity; it is evaluated by statistical methods (type A) or by other methods (type B), it has no known sign and is usually assumed to be symmetrical.

The error of measurement is the difference between the measured value of a quantity and the ‘true value’ of that quantity. An error has both a numerical value and a sign. Typically, the measurement errors are not known exactly, but they are estimated in the best possible way and corrections are made for them. After application of all known corrections, the expectation value for errors should be zero and the only quantities of concern are the uncertainties.

### 2.2.2.1.1 Type A standard uncertainty

If a measurement of a dosimetric quantity  $x$  is repeated  $N$  times, then the best estimate for  $x$  is  $x$  arithmetic mean value of all measurements  $x_i$ :

$$\bar{x} = \frac{1}{N} \sum_{i=1}^N x_i . \quad 2.2.1$$

The standard deviation  $\sigma_x$  characterizes the average uncertainty for an individual result  $x_i$  and is given by:

$$\sigma_x = \sqrt{\frac{1}{N-1} \sum_{i=1}^N (x_i - \bar{x})^2} . \quad 2.2.2$$

The standard deviation of the mean value is given by:

$$\sigma_{\bar{x}} = \frac{1}{\sqrt{N}} \sigma_x = \sqrt{\frac{1}{N(N-1)} \sum_{i=1}^N (x_i - \bar{x})^2} . \quad 2.2.3$$

The standard uncertainty of type A, denoted  $u_A$ , is defined as the standard deviation of the mean value,  $u_A = \sigma_{\bar{x}}$ . The standard uncertainty of type A is

obtained by a statistical analysis of repeated measurements and, in principle, it can be reduced by increasing the number of measurements.

### 2.2.2.1.2 Type B standard uncertainties

Type B standard uncertainties  $u_B$  cannot be estimated by repeated measurements, rather, they are intelligent guesses or scientific judgment of non-statistical uncertainties associated with the measurement. They include influences on the measuring process, application of correction factors or physical data taken from the literature. It is often assumed that type B standard uncertainties have a probability distribution, such as a normal (Gaussian) or a rectangular distribution (equal probability anywhere within the given limits). Type B standard uncertainty can be derived by estimating the limit, beyond which the value of the factor is not going to lie, and a fraction of this limit is taken as  $u_B$ . The fraction is chosen according to the distribution assumed.

### 2.2.2.1.3 Combined and expanded uncertainties

The equation that determines a dosimetric quantity  $Q$  at a point  $P$  is of the type:

$$Q_P = M \prod_{i=1}^N F_i , \quad 2.2.4$$

where  $M$  is the reading provided by the dosimetry system and  $F_i$  are the correction or conversion factors contained in the Eq. (2.2.4). The combined standard uncertainty,  $u_C$ , associated with the quantity  $Q$  is a quadratic summation of type A ( $u_A$ ) and type B ( $u_B$ ) uncertainties:

$$u_C = \sqrt{u_A^2 + u_B^2} . \quad 2.2.5$$

The combined uncertainty is assumed to exhibit a normal distribution and is multiplied by a coverage factor, denoted by  $k$ , to obtain the expanded uncertainty,  $U = k u_c$ . The result of the measurement of the quantity  $Q$  is then expressed by  $Q_p \pm U$ . The expanded uncertainty  $U$  with the coverage factor  $k = 2$ , corresponding to the 95% confidence level, is often used to represent the “overall uncertainty” which relates to the accuracy of the measurement of the quantity  $Q$ .

#### **2.2.2.1.4 Linearity**

Ideally, the dosimeter reading  $M$  should be linearly proportional to the dosimetric quantity  $Q$ . However, beyond a certain dose range a non-linearity sets in. The linearity range and the non-linearity behavior depend on the type of dosimeter and its physical characteristics. Two typical examples of response characteristics of dosimetry systems are sketched in Fig. 2.2.1 Curve A first exhibits linearity with dose, then a supralinear behavior, and finally saturation. Curve B first exhibits linearity and then saturation at high doses. In general, a non-linear behavior should be corrected for. A dosimeter and its reader may both exhibit non-linear characteristics but their combined effect could produce linearity over a wider range.

#### **2.2.3 Dose rate dependence**

Integrating systems measure the integrated response of a dosimetry system. For such systems the measured dosimetric quantity should be independent of the rate of that quantity. Ideally, the response of a dosimetry system,  $M/Q$ , at two different dose rates:  $(dQ/dt)_1$  and  $(dQ/dt)_2$  should remain constant. In reality, dose rate may influence the dosimeter readings and the appropriate corrections are necessary, e.g., recombination corrections for ionization chambers in pulsed beams.

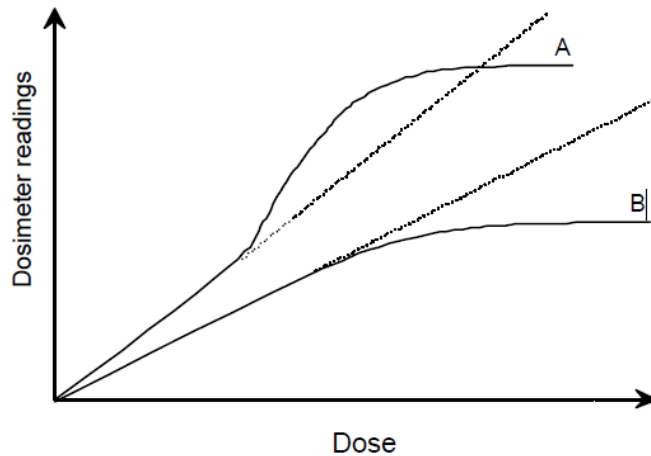


**FIG. 2.2.1. Response characteristics of two dosimetry systems. Curve A first exhibits linearity with dose, then supra linear behavior, and finally saturation. Curve B first exhibits linearity and then saturation at high doses.**

### **2.2.3.1 Energy dependence**

The response of a dosimetry system,  $M/Q$ , is generally a function of radiation beam quality (energy). Since the dosimetry systems are calibrated at a specified radiation beam quality (or qualities) and used over a much wider energy range, the variation of the response of a dosimetry system with radiation quality (called energy dependence) should be corrected for. Ideally, the energy response should be flat, i.e., the system calibration should be independent of energy over a certain range of radiation qualities. In reality, the energy correction has to be included in the determination of the quantity  $Q$  for most measurement situations. In radiotherapy, the quantity of interest is the dose to water (or to tissue). As no dosimeter is water or tissue equivalent for all radiation beam qualities, the energy dependence is an important characteristic of a dosimetry system.

## **Directional dependence**

The variation in response of a dosimeter with the angle of incidence of radiation is known as the directional, or angular, dependence of the dosimeter. Dosimeters usually exhibit directional dependence due to their constructional details, physical size, and the energy of the incident radiation. Directional dependence is important in certain applications, e.g., in in-vivo dosimetry while using semiconductor dosimeters. Therapy dosimeters are generally used in the same geometry as that in which they are calibrated.

### **2.2.3.2 Spatial resolution and physical size**

Because the dose is a point quantity, the dosimeter should allow the determination of the dose from a very small volume, i.e., one needs a 'point dosimeter' to characterize the dose at a point. TLD dosimeters come in very small dimensions and their use, to a great extent, approximates a point measurement. Film dosimeters have excellent 2D and gels 3D resolution, where the 'point' measurement is limited only by the resolution of the evaluation system. Ionisation chamber-type dosimeters, on the other hand, are of finite size to give the required sensitivity, although the new type of pin-point micro-chambers partially overcomes the problem. The position of the point where the dose is determined, i.e., its spatial location should be well defined in a reference co-ordinate system.



- **Readout convenience**

Direct-reading dosimeters (e.g., ionisation chambers) are generally more convenient than passive dosimeters; i.e., the ones that are read after due processing following the exposure (e.g., TLDs, films, etc.). While some dosimeters are inherently of the “integrating” type (e.g., TLDs, gel), others can measure in both integral and differential modes (ionisation chambers).

- . **Convenience of use**

Semiconductor dosimeters are reusable but with a gradual loss of sensitivity. Some dosimeters are not reusable at all (e.g., film, gel and alanine). Some dosimeters measure dose distribution in a single exposure (e.g., films, gels). Some dosimeters are quite rugged (i.e., handling will not influence sensitivity, e.g., ionization chambers), while others are sensitive to handling (e.g., TLDs).

## **2.2.4 FILM DOSIMETRY**

### **2.2.4.1. Radiographic film**

Radiographic x-ray film performs several important functions in diagnostic radiology, radiation therapy, and radiation protection. It can serve as radiation detector, relative dosimeter, a display device, and archival medium. Unexposed x-ray film consists of a base of thin plastic with a radiation sensitive emulsion (silver bromide AgBr grains suspended in gelatin) coated uniformly on one or both sides of the base. Ionization of AgBr in the grains, as a result of radiation

interaction, forms the latent image in the film. Image becomes visible (film blackening) only after development.

Light transmission is a function of the film opacity and can be measured in terms of optical density (OD) with special devices called densitometers. Optical density is defined as  $OD = \log_{10} (I_0/I)$  and is a function of dose.  $I_0$  is the initial light intensity and  $I$  is the intensity transmitted through the film. Film gives excellent 2D spatial resolution and, in a single exposure, it provides information about the spatial distribution of radiation in the area of interest or the attenuation of radiation by objects. Useful dose range of film is limited; energy dependence is pronounced for lower energy photons, and the response depends on several, difficult to control, parameters. Typically, films are used for qualitative dosimetry but with proper calibration, careful use and analysis, film can also be used for dose evaluation.

Various types of films are available for radiotherapy work (e.g., direct exposure non-screen films for field size verification, phosphor screen films used with simulators, metallic screen films used in portal imaging, etc.). Unexposed film would exhibit a background optical density called the fog density ( $OD_f$ ). The density due to radiation exposure called the net optical density can be obtained from the measured density by subtracting the fog density. The OD readers are film densitometers, laser densitometers, automatic film scanners, etc. The principle of operation of a simple film densitometer is shown in Fig. 3.6.

Ideally, the relationship between the dose and OD should be linear, but unfortunately this is not always the case. Some emulsions are linear, some are linear over a limited dose range and others are non-linear. So the dose vs. OD curve, known as the sensitometric curve (also known as the characteristic or H&D curve, in honor of Hurter and Driffield who first investigated the relationship) must be established for each film before using it for dosimetry work.

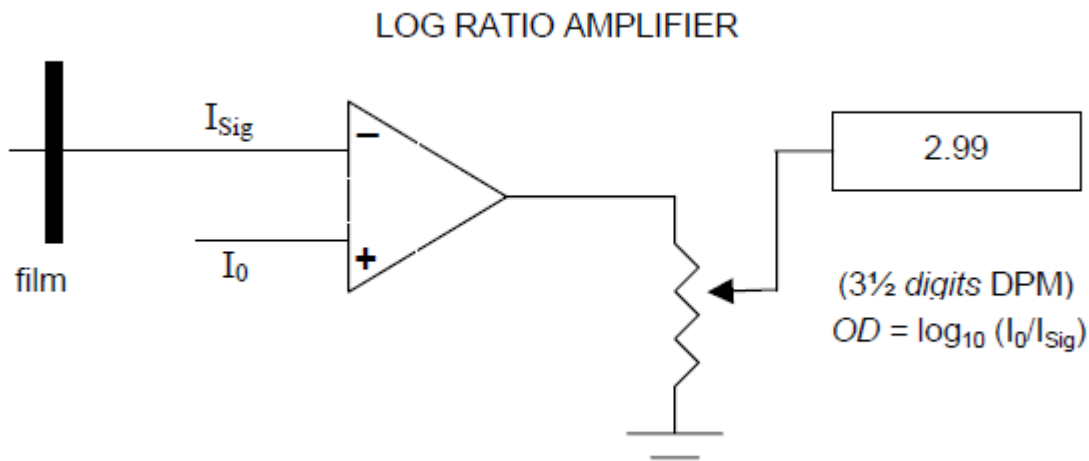


**FIG. 2.2.2. Schematic diagram of a basic film densitometer.**

referred to as optimum measurement conditions; the toe is the region A typical H&D curve for a radiographic film is shown in Fig. 2.2.7. It has four regions: (1) fog, at low or zero exposures; (2) toe; (3) linear portion at intermediate exposures; and (4) shoulder and saturation at high exposures. The linear portion is of underexposure, and the shoulder as the region of overexposure.

Important parameters of film response to radiation are: gamma, latitude and speed.

The slope of the straight line portion of the H&D curve is called the gamma of the film. The exposure should be chosen to make all parts of the radiograph lie on the linear portion of the H&D curve to ensure the same contrast for all optical densities.

The latitude is defined as the range of exposures over which the densities will lie in the linear region. Speed of a film is determined by giving the exposure required to produce an optical density of 1.0 greater than the OD of fog. Typical applications of a radiographic film in radiotherapy are qualitative and quantitative measurements, including electron beam dosimetry, quality control of radiotherapy machines (e.g., congruence of light and radiation fields, determination of the position of a collimator axis, so called star test), verification of treatment techniques in various phantoms and portal imaging.

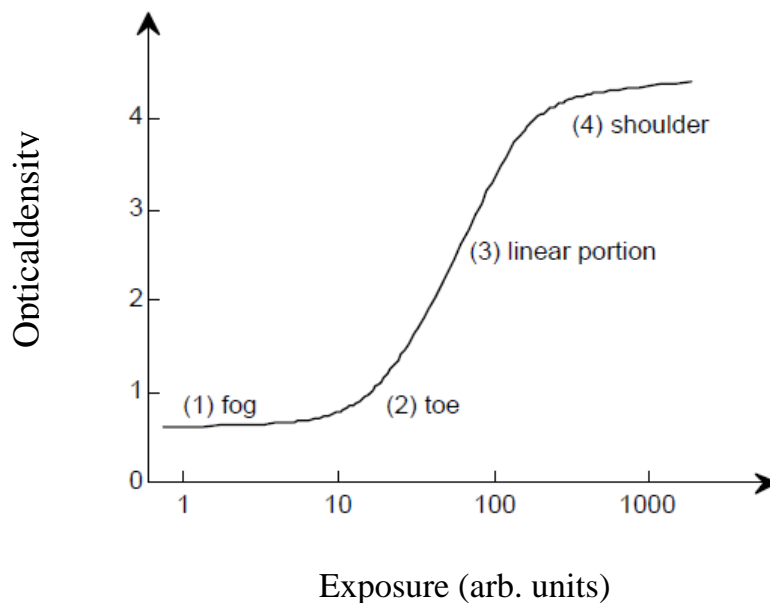


**FIG. 2.2.3. Typical sensitometric (characteristic H&D) curve for a radiographic film.**

#### **2.2.4.2. Radiochromic film**

Radiochromic film is a new type of film in radiotherapy dosimetry. The most commonly used is a Gaf Chromic<sup>TM</sup> film. It is a colorless film with a nearly tissue equivalent composition (H 9.0%, C 60.6%, N 11.2%, and O 19.2%) that develops a blue color upon radiation exposure.

Radiochromic film contains a special dye that gets polymerized upon exposure to radiation. The polymer absorbs light and the transmission of light through the film can be measured with a suitable densitometer. Radiochromic film is self-developing, needs neither developer nor fixer.

Since the radio chromic film is grain less, it has a very high resolution and can be used in high dose gradient regions for dosimetry, e.g., near brachytherapy sources, in measurement of dose distributions in stereotactic fields, etc.

The dosimetry with GafChromic films has a few advantages over the radiographic films, such as the ease of use, not requiring dark rooms, film cassettes or film processing; dose rate independence; better energy characteristics except for low energy x rays (25 kV); insensitivity to ambient conditions (although excessive humidity should be avoided). Gaf Chromic films are generally less sensitive than radiographic films and are useful at higher doses, although the dose-response non-linearity should be corrected for in the upper dose region. Radiochromic film is a relative dosimeter; it is possible to achieve the precision better than 3%, if proper care is taken of its calibration and with the environmental conditions. Data

on the various characteristics of Gaf Chromic films (e.g., sensitivity, linearity, uniformity, reproducibility, post-irradiation stability, etc.) are available in the literature.

### **2.2.5. LUMINESCENCE DOSIMETRY**

Some materials, upon absorption of radiation, retain part of the absorbed energy in metastable states. When this energy is subsequently released in the form of ultraviolet, visible or infrared light, the phenomenon is called as luminescence.

Two types of luminescence: fluorescence and phosphorescence, are known depending on the time delay between the stimulation and the emission of light.

Fluorescence occurs with a time delay between  $10^{-10}$  to  $10^{-8}$  seconds; phosphorescence with a time delay exceeding  $10^{-8}$  seconds. The process of phosphorescence can be accelerated with a suitable excitation in the form of heat or light. If the exciting agent is heat, the phenomenon is known as thermoluminescence and the material is called a thermoluminescent (TL) material or a thermoluminescent dosimeter (TLD) when used for purposes of dosimetry. If the exciting agent is light, the phenomenon is referred to as optically stimulated luminescence (OSL).

As discussed in Section 1.4., the highly energetic secondary charged particles, usually electrons that are produced in the primary interactions of photons with matter are mainly responsible for the photon energy deposition in matter. In a

crystalline solid these secondary charged particles release numerous low energy free electrons and holes through ionizations of atoms and ions. The free electrons and holes thus produced will either recombine or become trapped in an electron or hole trap, respectively, somewhere in the crystal.

The traps can be intrinsic or can be introduced in the crystal in the form of lattice imperfections consisting of vacancies or impurities. Two types of traps are known in general: storage traps and recombination centers.

A storage trap merely traps free charge carriers and releases them during the subsequent (i) heating resulting in the TL process or (ii) irradiation with light resulting in the OSL process.

A charge carrier released from a storage trap may recombine with a trapped charge carrier of opposite sign in a recombination center (luminescence center). The recombination energy is at least partially emitted in the form of ultraviolet, visible or infrared light that can be measured with photodiodes or photomultiplier tubes.

#### **2.2.5.1. Thermoluminescence**

Thermoluminescence (TL) is thermally activated phosphorescence; the most spectacular and the most widely known of a number of different ionizing radiation induced thermally activated phenomena. Its practical applications range from archeological pottery dating to radiation dosimetry. In 1968 Cameron,

Suntharalingam and Kenney published a book on the TL process that is still considered an excellent treatise on the practical aspects of the TL phenomenon.

A useful phenomenological model of the TL mechanism is provided in terms of the band model for solids. The storage traps and recombination centers, each type characterized with an activation energy (trap depth) that depends on the crystalline solid and the nature of the trap, are located in the energy gap between the valence band and the conduction band. The states just below the conduction band represent electron traps, the states just above the valence band are hole traps. The trapping levels are empty before irradiation, i.e., the hole traps contain electrons and the electron traps do not.

During the irradiation the secondary charged particles lift electrons into the conduction band either from the valence band (leaving a free hole in the valence band) or from an empty hole trap (filling the hole trap).

The system may approach thermal equilibrium through several means:

- (1) Free charge carriers recombine with the recombination energy converted into heat.
- (2) A free charge carrier recombines with a charge carrier of opposite sign trapped at a luminescence center, the recombination energy being emitted as optical fluorescence.
- (3) The free charge carrier becomes trapped at a storage trap, and this event is then responsible for phosphorescence or the TL and OSL processes.



### 2.2.5.2. TLD systems

TL dosimeters most commonly used in medical applications are LiF:Mg,Ti, LiF:Mg,Cu,P and  $\text{Li}_2\text{B}_4\text{O}_7\text{:Mn}$ , because of their tissue equivalence. Other TLDs, used because of their high sensitivity, are  $\text{CaSO}_4\text{:Dy}$ ,  $\text{Al}_2\text{O}_3\text{:C}$  and  $\text{CaF}_2\text{:Mn}$ . TLDs are available in various forms (e.g., powder, chips, rods, ribbon, etc.). Before they are used, TLDs have to be annealed to erase the residual signal. Well-established reproducible annealing cycles should be used including the heating and cooling rates.

A basic TLD reader system consists of a planchet for placing and heating the TLD dosimeter; a photomultiplier tube (PMT) to detect the TL light emission, convert it into an electrical signal, and amplify it; and an electrometer for recording the PMT signal as charge or current. A basic schematic diagram of a TLD reader is shown in Fig. 3.8. The TL intensity emission is a function of the TLD temperature  $T$ . Keeping the heating rate constant makes the temperature  $T$  proportional to time  $t$  and so the TL intensity can be plotted as a function of  $t$  if a recorder output is available with the TLD measuring system. The resulting curve is called the TLD glow curve (Fig. 3.9). In general, if the emitted light is plotted against the crystal temperature one obtains a TL thermogram. The peaks in the glow curve may be correlated with trap depths responsible for TL emission. The main dosimetric peak of the LiF:Mg,Ti glow curve between  $180^\circ$  and  $260^\circ\text{C}$  is used for dosimetry. The peak temperature is high enough for not being affected

by room temperature and still low enough so as not to interfere with black-body emission from the heating planchet.

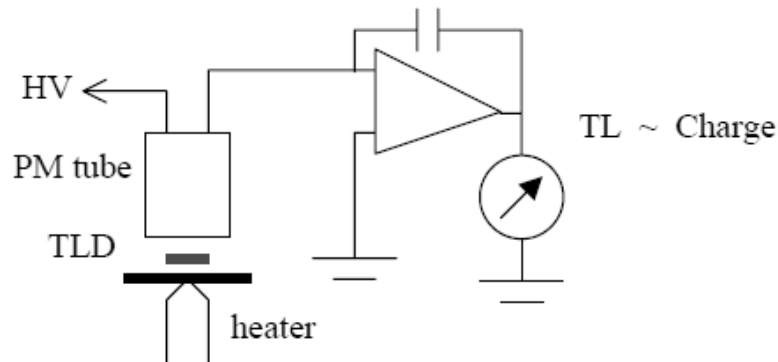


**FIG. 2.2.4 Schematic diagram of a TLD reader.**

The total TL signal emitted, i.e., the area under the appropriate portion of the glow curve, can be correlated to dose through proper calibration. Good reproducibility of heating cycles during the readout is important for accurate dosimetry. TL signal decreases in time after the irradiation due to spontaneous emission of light at room temperature. This process is called fading. Typically, for LiF:Mg,Ti, the fading of the dosimetric peak does not exceed a few percent per year. TL dose response is linear over a wide range of doses used in radiotherapy, although it increases in higher dose region exhibiting supralinear behaviour before it saturates at even higher doses. TL dosimeters have to be calibrated before they are used (thus they serve as relative dosimeters). To derive the absorbed dose from the TL-reading a few correction factors have to be applied, such as energy correction, fading and dose-response non-linearity

corrections. Typical applications of TLD in radiotherapy are: in vivo dosimetry on patients (either as a routine QA procedure or for dose monitoring in special cases, e.g., complicated geometries, dose to critical organs, total body irradiation, in brachytherapy, etc.), verification of treatment techniques in various phantoms (e.g., Rando phantom), dosimetry audits (such as the IAEA/WHO TLD postal dose audit programme) and comparisons among hospitals.

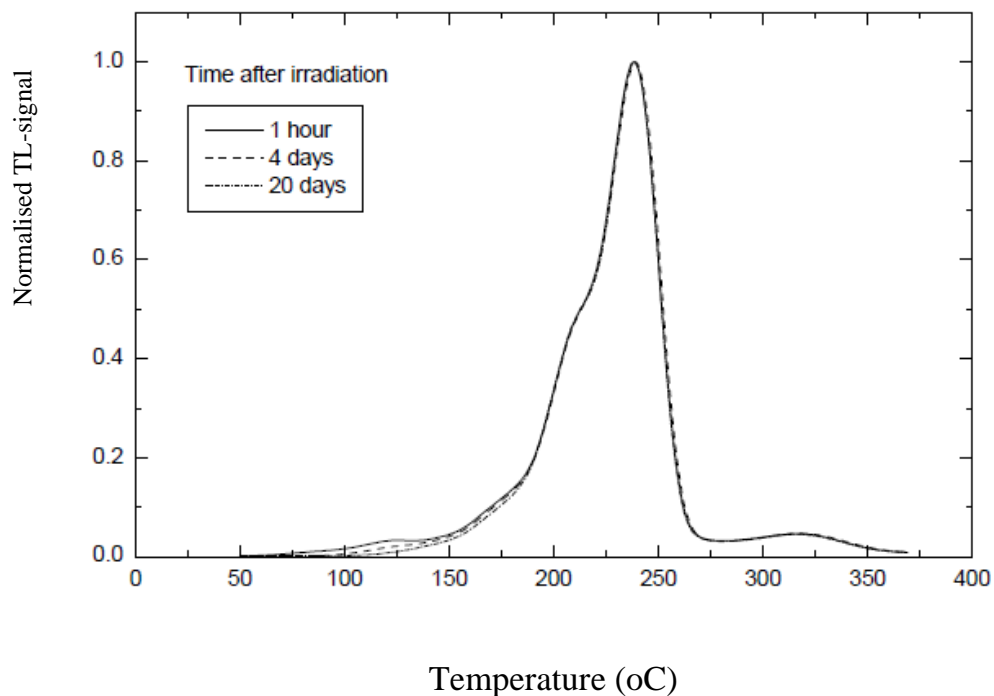


**Fig. 2.2.5. A typical glow-curve (thermogra) of LiF:Mg,Ti measured with a TLD reader at a low heating rate.**

### 2.2.5.3. OSL systems

Optically-stimulated luminescence (OSL) is based on a principle similar to that of the TLD. Instead of heat, light (from a laser) is used to release the trapped energy in the form of luminescence. OSL is a novel technique offering a potential for in vivo dosimetry in radiotherapy. The integrated dose measured during irradiation can be evaluated using OSL directly afterwards. The optical fiber OSL dosimeter consist of a small ( $\sim 1 \text{ mm}^3$ ) chip of carbon-doped aluminum oxide ( $\text{Al}_2\text{O}_3:\text{C}$ ) coupled with a long optical fiber, a laser, a beam-splitter and a collimator, a PM tube, electronics and software. To produce OSL, the chip is excited with a laser light through an optical fiber and the resulting luminescence (blue light) is carried back in the same fiber, reflected through a  $90^\circ$  by the beam-splitter and measured in a PMT.

The optical fiber dosimeter exhibits high sensitivity over the wide range of dose rates and doses used in radiotherapy. The OSL response is generally linear and independent of energy as well as the dose rate, although the angular response requires correction.

Various experimental set-ups exist, such as pulsed OSL or OSL used in conjunction with RL (radio-luminescence). RL is emitted promptly at the time of dosimeter irradiation and provides information on the dose rate during irradiation while the OSL provides the integrated dose thereafter. This technique, although

not yet used routinely in radiotherapy, may prove to be a valuable tool for in vivo dosimetry in the future.

## **2.2.6. SEMICONDUCTOR DOSIMETRY**

### **2.2.6.1. Silicon diode dosimetry systems**

Silicon diode dosimeter is a p-n junction diode. The diodes are produced by taking n-type or p-type silicon and counter-doping the surface to produce the opposite type material. These diodes are referred to as n-Si or p-Si dosimeters, depending upon the base material. Both types of diodes are commercially available, but only the p-Si type is suitable for radiotherapy dosimetry, since it is less affected by radiation damage and has a much smaller dark current. Radiation produces electron-hole (e-h) pairs in the body of the dosimeter including the depletion layer. The charges (minority carriers) produced in the body of the dosimeter, within the diffusion length, diffuse into the depleted region. They are swept across the depletion region under the action of the electric field due to the intrinsic potential. In this way a current is generated in the reverse direction in the diode. Diodes are used in the short circuit mode, since this mode exhibits a linear relationship between the measured charge and dose. They are usually operated without an external bias to reduce leakage current. Diodes are more sensitive and smaller in size compared to typical ionization chambers. They are relative dosimeters and should not be used for beam calibration, since their sensitivity changes with repeated use due to radiation damage. Diodes are particularly useful

for measurement in phantoms, e.g., small fields used in stereotactic radiosurgery or high dose gradient areas such as the penumbra region. They are also often used for measurements of depth doses in electron beams. For the use with beam scanning devices in water phantoms, they are packaged in a waterproof encapsulation. When used in electron beam depth dose measurements, diodes measure directly the dose distribution (in contrast to the ionization measured by ionization chambers).

Diodes are widely used in routine in-vivo dosimetry on patients or for bladder or rectum dose measurements. Diodes for in vivo dosimetry are provided with build-up encapsulation and hence must be appropriately chosen, depending on the type and quality of the clinical beams. The encapsulation also protects the fragile diode from physical damage.

When diodes are used for in vivo dosimetry, they have to be calibrated and several correction factors have to be applied for dose calculation. The sensitivity of diodes depends on their radiation history, so the calibration has to be repeated periodically.

Diodes show a variation in dose response with temperature (particularly important for long treatments), dependence of signal on the dose rate (care should be taken for different source-skin distances), angular (directional) dependence and energy dependence even for small variation in the spectral composition of radiation beams (important for the measurement of entrance and exit doses).

### **2.2.6.2. MOSFET dosimeter**

The Metal-Oxide Semiconductor Field Effect Transistor (MOSFET), a miniature silicon transistor, seems to be a promising candidate for medical dosimetry. MOSFETs are small in size even compared to diodes, offering very little attenuation of the beam when used for in vivo dosimetry. They require a special read-out facility. A single dosimeter can cover the full energy range of photons and electrons, although the energy response should be examined, since it varies with radiation quality. Similarly to diodes, MOSFETs exhibit a temperature dependence. As they show non-linearity of response with total absorbed dose, regular sensitivity checks are required. MOSFETs are also sensitive to changes in the bias voltage during irradiation (it must be stable) and their response drifts slightly after the irradiation (the reading must be taken in a specified time after exposure). They have a limited life-span.

MOSFETs have been in use for the past few years in radiotherapy applications, such as surface dose measurements, radiosurgery, in vivo dosimetry, and brachytherapy measurements.

## **2.2.7. OTHER DOSIMETRY SYSTEMS**

### **2.2.7.1. Alanine/EPR dosimetry system**

Alanine, one of the amino acids, pressed in the form of rods or pellets with an inert binding material, is typically used for high dose dosimetry. The dosimeter can be used at the level of about 10 Gy or more with sufficient precision for

radiotherapy dosimetry. The radiation interaction results in the formation of alanine radicals, the concentration of which can be measured using an electron paramagnetic resonance (EPR), known also as electron spin resonance (ESR), spectrometer. The intensity is measured as the peak-to-peak height of the central line in the spectrum. The readout is non-destructive. Alanine is tissue-equivalent and it requires no energy correction within the quality range of typical therapeutic beams. It exhibits very little fading for many months after irradiation. The response depends on environmental conditions during irradiation (temperature) and storage (humidity). At present, alanine's potential application for radiotherapy is in dosimetry comparisons among hospitals.

#### **2.2.7.2. Plastic scintillator dosimetry system**

Plastic scintillators are a relatively new development in radiotherapy dosimetry. The light generated in the scintillator during its irradiation is carried away by an optical fiber to a PMT located outside the irradiation room. A typical setup requires two sets of optical fibers which are coupled to two different PMTs, allowing subtraction of the background Cerenkov radiation from the measured signal. Response of the scintillation dosimeter is linear in the dose range of therapeutic interest.

Plastic scintillators are almost water-equivalent in terms of electron density and atomic composition. Typically, they match the water mass stopping power and mass energy absorption coefficient to within  $\pm 2\%$  for the range of beam energies



in clinical use including the kV region. Scintillators are nearly energy independent and can thus be used directly for relative dose measurements.

Dosimeter can be made very small (about 1 mm<sup>3</sup> or less) and yet give adequate sensitivity for clinical dosimetry. Hence, it can be used in cases where high spatial resolution is required (e.g., high dose gradient regions, buildup regions, interface regions, small field dosimetry, doses very near to brachytherapy sources, etc.).

Due to flat energy dependence and small size, plastic scintillators are ideal dosimeters for brachytherapy applications.

Dosimetry based on plastic scintillators is characterized with good reproducibility and long term stability. Scintillators suffer no significant radiation damage (up to about 10 kGy) although the light yield should be monitored when used clinically.

Plastic scintillators are independent of dose rate and can be used from 10 μGy/min (ophthalmic plaque dosimetry) to about 10 Gy/min (external beam dosimetry).

They have no significant directional dependence and need no ambient temperature or pressure corrections.

### **2.2.7.3. Diamond dosimeters**

Diamonds change their resistance upon radiation exposure. When applying a bias voltage, the resulting current is proportional to the dose rate of radiation.

Commercially-available diamond dosimeters are designed to measure relative dose distributions in high energy photon and electron beams. The dosimeter is

based on a natural diamond crystal sealed in polystyrene housing with a bias applied through thin golden contacts. Diamonds have a small sensitive volume, on the order of a few  $\text{mm}^3$ , which allows the measurement of dose distributions with an excellent spatial resolution. Diamond dosimeters are tissue-equivalent and require nearly no energy correction. Thanks to a flat energy response, small physical size and negligible directional dependence diamonds are well suited for the use in high dose gradient regions, e.g., for stereotactic radiosurgery.

- In order to stabilize their dose response, diamonds should be irradiated prior to each use to reduce the polarization effect. They exhibit some dependence of the signal on the dose rate that has to be corrected for when measuring e.g. depth doses. Also, they have an insignificant temperature dependence on the order  $0.1\% \text{ } ^\circ\text{C}^{-1}$  or less.

- High sensitivity and resistance to radiation damage are other important features of the diamond dosimeter. It is waterproof and can be used for measurements in a water phantom.

#### **2.2.7.4. Gel dosimetry systems**

Gel dosimetry systems are the unique true 3D dosimeters suitable for relative dose measurements. The dosimeter is at the same time a phantom that can measure absorbed dose distribution in a full 3D geometry. Gels are nearly tissue-equivalent and can be shaped to any desirable shape or form. Gel dosimetry can be divided in two types:

- Fricke gels based on the well-established Fricke dosimetry and

- Polymer gels. In Fricke gels,  $\text{Fe}^{2+}$  ions in ferrous sulfate solutions are dispersed throughout gelatine, agarose or PVA matrix. Radiation induced changes are either due to direct absorption of radiation or via intermediate water free radicals. Upon radiation exposure ferrous ions  $\text{Fe}^{2+}$  are converted into ferric ions  $\text{Fe}^{3+}$  with a corresponding change in paramagnetic properties that may be measured using Nuclear Magnetic Resonance (NMR) relaxation rates or optical techniques. A 3D image of the dose distribution is created. A major limitation of the Fricke gel systems is the continual post-irradiation diffusion of ions resulting in a blurred dose distribution. In polymer gel monomers such as acrylamid are dispersed in a gelatine or agarose matrix. Upon radiation exposure, monomers undergo a polymerization reaction resulting in a 3D polymer gel matrix which is a function of absorbed dose that can be evaluated using NMR, x-ray computer tomography, optical tomography, vibrational spectroscopy or ultrasound. A number of various polymer gel formulations are available including polyacryl-amide gels generally referred as PAG gels (e.g., BANG<sup>TM</sup> gel) and the new normoxic gels (e.g., MAGIC gel); the latter are not sensitive to the presence of atmospheric oxygen. There is a semi-linear relationship between the NMR relaxation rate and the absorbed dose at a point in the gel dosimeter. Hence, by mapping the relaxation rates using an NMR scanner, the dose map can be derived by computation and by proper calibration. Due to a large proportion of water, polymer gels are nearly

water-equivalent and no energy corrections are required for photon and electron beams used in radiotherapy.

No significant dose rate effects in polymer gels have been observed using NMR evaluation, although dose response depends on temperature at which the dosimeter is evaluated. The strength of the magnetic field during evaluation may also influence the dose response. Care should be taken of post-irradiation effects such as continual polymerization, gelation and strengthening of the gel matrix that may lead to the image distortion.

Gel dosimetry is a highly promising relative dosimetry technique that may prove particularly useful for dose verification in complex clinical situations (e.g., intensity modulated radiotherapy), in anatomically shaped phantoms, and for evaluation of doses in brachytherapy, including cardiovascular brachytherapy.

#### **2.2.8. PRIMARY STANDARDS**

Primary standards are instruments of the highest metrological quality that permit determination of the unit of a quantity from its definition, the accuracy of which has been verified by comparison with standards of other institutions of the same level. Primary standards are realized by the Primary Standards Dosimetry Laboratories (PSDLs) in about twenty countries world-wide. Regular international comparisons between the PSDLs, and with the Bureau International des Poids et Mesures (BIPM), ensure international consistency of the dosimetry standards.

Ionisation chambers used in hospitals for calibration of radiation therapy beams must have a calibration traceable (directly or indirectly) to a primary standard. Primary standards are not used for routine calibrations, since they represent the unit for the quantity at all times. Instead, the PSDLs calibrate secondary standard dosimeters for Secondary Standard Dosimetry Laboratories (SSDLs) that in turn are used for calibrating the reference instruments of users, such as therapy level ionisation chambers used at hospitals.

#### **2.2.8.1. Primary standard for air-kerma in air**

Free-air ionisation chambers are the primary standard for air-kerma in air for superficial and orthovoltage x-rays (up to 300 kV). They cannot function as a primary standard for cobalt-60 beams, since the air column surrounding the sensitive volume (for establishing the electronic equilibrium condition in air) would become very long. This would make the chamber very bulky and the various required corrections and their uncertainties would also become problematic. At cobalt-60 energy graphite cavity ionisation chambers with accurately known chamber volume are used as the primary standard. The use of the graphite cavity chamber is based on the Bragg-Gray cavity theory.

#### **2.2.8.2. Primary standards for absorbed dose-to-water**

The standards for absorbed dose to water enable therapy level ionisation chambers to be calibrated directly in terms of absorbed dose to water instead of air-kerma in air. This simplifies the dose determination procedure at a hospital

level and improves the accuracy compared to the air-kerma-based formalism. Standards for absorbed dose to water calibration are now available for cobalt-60 beams in several PSDLs and some have extended their calibration services to high energy photon and electron beams from accelerators.

Ideally, the primary standard for absorbed dose to water should be a water calorimeter that would be an integral part of a water phantom and would measure the dose under reference conditions. However, difficulties in the establishment of this standard have led to the development of primary standard of absorbed dose in various different ways.

At present there are three basic methods used for the determination of absorbed dose to water at the primary standard level. These are: ionometric method, total absorption method based on chemical dosimetry and calorimetry.

#### **2.2.8.3. Ionometric standard for absorbed dose-to-water**

Graphite cavity ionisation chamber with accurately known active volume, constructed as a close approximation to a Bragg-Gray cavity, is used in a water phantom at a reference depth. Absorbed dose to water at the reference point is derived from the cavity theory using the mean specific energy imparted to the air in the cavity and the restricted stopping power ratio of the wall material to the cavity gas. BIPM maintains an ionometric standard of absorbed dose to water.

#### 2.2.8.4. Chemical dosimetry standard for absorbed dose-to-water

In chemical dosimetry systems the dose is determined by measuring the chemical change produced in the medium (the sensitive volume of the dosimeter) using a suitable measuring system. The most widely used chemical dosimetry standard is the Fricke dosimeter. The Fricke solution has the following composition: 1 mM  $\text{FeSO}_4$  or  $\text{Fe}(\text{NH}_4)_2(\text{SO}_4)_2$  + 0.8 N  $\text{H}_2\text{SO}_4$  air saturated + 1 mM NaCl. Irradiation of Fricke solution oxidizes ferrous ions  $\text{Fe}^{2+}$  into ferric ions  $\text{Fe}^{3+}$ ; the latter exhibit a strong absorption peak at  $\lambda = 304$  nm, whereas ferrous ions do not show any absorption at this wavelength. Radiation induced ferric ion concentration can be determined using spectro-photometry, which measures the absorbance (in optical density units) of the solution. Fricke dosimeter response is expressed in terms of its sensitivity, known as the radiation chemical yield, G-value, and defined as the number of moles of ferric ions produced per joule of the energy absorbed in the solution. Chemical dosimetry standard is realized by the calibration of a transfer dosimeter, in a total absorption experiment and the subsequent application of the transfer dosimeter in a water phantom, in reference conditions. The response of the Fricke solution is determined first using the total absorption of an electron beam. An accurate determination of the energy response of the transfer instrument is necessary, i.e., knowing the electron energy, the beam current and the absorbing mass accurately, the total absorbed energy can be determined and related to the change in absorbance of the Fricke solution. Next, the absorbed

dose to water at the reference point in a water phantom is obtained using the Fricke dosimeter as the transfer dosimeter.

#### **2.2.8.5. Calorimetric standard for absorbed dose-to-water**

Calorimetry is the most fundamental method of realizing the primary standard for absorbed dose, since temperature rise is the most direct consequence of energy absorption in a medium. Graphite is in general an ideal material for calorimetry, since it is of low atomic number  $Z$  and all the absorbed energy reappears as heat, without any loss of heat in other mechanisms (such as the heat defect). The graphite calorimeter is used by several PSDLs to determine the absorbed dose to graphite in a graphite phantom. The conversion to absorbed dose to water at the reference point in a water phantom may be performed by an application of the photon fluence scaling theorem or by measurements based on cavity ionization theory. Graphite calorimeters are electrically calibrated by depositing a known amount of electrical energy into the core. Water calorimeters offer a more direct determination of the absorbed dose to water at the reference point in a water phantom. The absorbed dose to water is derived from the measured temperature rise at a point in water relying on an accurate knowledge of the specific heat capacity. No scaling laws are required as is the case in graphite calorimetry. However, there are technical complications related to a heat defect due to water radiolysis and heat transport, which need to be corrected for.



Water calorimeters are calibrated through the calibration of their thermistors in terms of the absolute temperature difference rather than through the energy depositing as it is the case of graphite calorimeters.

### **2.2.9. Summary of some commonly used dosimetric systems**

Radiation dosimeters and dosimetry systems come in many shapes and forms, and they rely on numerous physical effects for storage and readout of the dosimetric signal. The four most commonly used radiation dosimeters are:

- (1) Ionization chamber
- (2) Radiographic film
- (3) Thermoluminescent dosimeter
- (4) Diode

The strengths and weaknesses of the four dosimeters are summarized in Table

2.2.I.

**Table 2.2.1 Main advantages and disadvantages of four commonly used dosimetric systems**

<b>Dosimeter</b>	<b>Advantages</b>	<b>Disadvantages</b>
<b>Ionisation chamber</b>	Accurate and precise Recommended for beam calibration Necessary corrections well understood Instant readout 2D spatial resolution	Connecting cables required High voltage supply required Many corrections required for high energy dosimetry Dark room, processing
<b>Film</b>	Very thin - does not perturb the beam	facilities required Processing difficult to control Variation between films and batches Needs proper calibration against ion chamber measurements Energy dependence problems Cannot be used for beam calibration
<b>TLD</b>	Small in size - point dose measurements possible Many TLDs can be exposed in single exposure Available in various forms Some are reasonably tissue equivalent Not expensive	Signal erased during readout Easy to lose reading No instant readout Accurate results require care Readout and calibration time consuming Not recommended for beam calibration
<b>Diode</b>	Small size High sensitivity Instant readout No external bias voltage Simple instrumentation	Requires connecting cables Variability of calibration with temperature Change in sensitivity with accumulated dose Special care needed to ensure constancy of response Cannot be used for beam calibration